Optimal Distributed Control of AC Microgrids with Coordinated Voltage Regulation and Reactive Power Sharing

Sheik M. Mohiuddin, Student Member, IEEE and Junjian Qi, Senior Member, IEEE

Abstract—In this paper, we propose an optimal distributed voltage control for grid-forming (GFM) inverters in islanded AC microgrids. An optimization problem is formulated where the distributed generator (DG) output voltage is considered as the control variable with technical constraints on voltage and reactive power output capacity and an objective function that makes a trade-off between voltage regulation and reactive power sharing. A distributed primal-dual gradient based algorithm is developed to solve the formulated optimization problem to address the challenges due to non-separable objective function, unavailable global average voltage, and globally coupled reactive power constraints. The effectiveness of the proposed optimal distributed control is validated through simulations on the 4-DG test microgrid and the modified IEEE 34-bus distribution test system, and the advantages of the proposed control over existing controls are demonstrated.

Index Terms—Distributed control, distributed optimization, optimal control, primal-dual gradient, reactive power sharing, secondary control, voltage regulation.

I. INTRODUCTION

THE proliferation of renewable energy resource-based distributed generation and its increased penetration into the power grid contribute to the rapid development of microgrids, in which the electric power generation, storage, and consumption occur in a predefined boundary by appropriate coordination among the tertiary, secondary, and primary control layers [1], [2]. A microgrid can operate either in islanded or grid-connected mode [3], [4]. In grid-connected mode the distributed generators (DGs) operate in grid-following mode and the voltage regulation of the distribution systems are performed through local reactive power control [5], [6]. In islanded mode the DG controllers are usually operated in grid-forming (GFM) mode in which the grid voltage and frequency are regulated by the DG controllers [7].

The primary control in a microgrid can be realized in a decentralized manner through the well-known droop control technique which ensures proportional power-sharing and voltage/frequency stability [8]–[10]. Albeit the operational simplicity and the characteristics of emulating synchronous generator behavior [9], droop control has some practical limitations such as deviation in steady-state voltage/frequency [11], poor

This work was supported by the National Science Foundation under Grant No. ECCS-2103426. Paper no. TSG-00429-2021. (Corresponding author: Junjian Oi.)

S. M. Mohiuddin and J. Qi are with the Department of Electrical and Computer Engineering, Stevens Institute of Technology, Hoboken, NJ 07030 USA (e-mails: smohiudd@stevens.edu; jqi8@stevens.edu).

dynamic performance in the presence of nonlinear loads [12], and inappropriate reactive power-sharing for the line voltage drop [11]. Alternatively, improved droop control techniques based on adaptive droop [13], [14] and optimized virtual impedance [15] have been proposed. However, in the presence of nonlinear/unbalance loads and unequal feeder impedances, the performance of these improved droop control techniques may deteriorate [16].

To compensate for the voltage/frequency deviations caused by the primary control, a secondary control with centralized or distributed communication architecture may be developed [9]. For global coordination, the centralized control requires a high-bandwidth two-way communication structure which incurs high computational burden and additional implementation costs [17]. Also, centralized schemes do not proliferate the "plug and play" feature in the microgrid and are susceptible to the single point of failure problem [3], [18]. By contrast, distributed control can overcome the limitation of the centralized control structure by utilizing a sparse communication network where each agent only has access to the information of a small number of neighboring agents [9], [19], reducing the computational complexity and increasing the resiliency [3], [9], [20], [21]. The convergence criteria of the distributed controllers have been widely investigated [22]-[25].

A key challenge for the distributed control of microgrids is to coordinate voltage regulation and reactive power sharing. An optimal distributed control with average voltage regulation and reactive power sharing is presented in [26]. Distributed adaptive virtual impedance (DAVI) [27] and distributed averaging proportional-integral (DAPI) [28] controls with average voltage regulation and reactive power sharing are also proposed. A reactive power sharing approach with event-triggered communication is discussed in [8]. The distributed controls proposed in [8], [26]–[28] require droop control in the primary level and thus have the aforementioned limitations. Droop-free distributed control with average voltage regulation is presented [9]. However, average voltage regulation alone cannot always guarantee admissible voltage profiles especially for heavily loaded operating conditions [3].

A containment and consensus based control to achieve reactive power sharing and bounded voltage regulation is presented in [29]. This control also depends on the droop-based primary control and only the leader DGs can access the voltage references. The authors in [11] propose a voltage bounding and reactive power regulation scheme. However, in this approach all DGs are connected to a common critical bus which may

not be suitable for networked microgrid structure [15]. In [3], a distributed control scheme is proposed that has an average voltage regulator, a voltage variance regulator, and relaxed reactive power sharing for an islanded microgrid. However, to achieve the control objectives a special DG is required which may have a large variation in reactive power sharing from the other DGs. Furthermore, the existing papers on the control of islanded microgrids have not systematically considered the technical constraints on voltage magnitude and reactive power output capacity of the DGs. Also, the distributed controls in the aforementioned literature extensively use PI controllers which may not always guarantee theoretical convergence.

From the aforementioned survey, it is evident that a generalized control framework is required for optimally coordinating voltage regulation and reactive power sharing objectives while obeying all necessary technical constraints. The authors in [30], [31] propose optimal distributed voltage control with limited communication among the neighboring agents where voltage and reactive power constraints are considered and an objective function to minimize the power loss and reactive power operation cost is defined. A hybrid voltage control strategy with limited communication is also proposed in [32]. However, the controls in [30]-[32] are developed using the linearized Distflow method of the radial distribution network and work with the grid-following inverters under grid-connected mode where reactive power from the DGs is considered as the control variable. In this paper, a generalized optimization problem is formulated for the GFM inverters in islanded AC microgrids. The main contributions of the paper are summarized as follows.

- An optimization problem is formulated for GFM inverters in AC microgrids for an optimal trade-off between voltage regulation and reactive power sharing, obeying technical constraints on DG output voltage and reactive power capacity. The problem is then converted to a convex optimization problem to facilitate computation.
- 2) A primal-dual gradient based distributed solving algorithm is developed to solve the formulated convex optimization problem distributedly and address unique challenges such as non-separable objective function, unavailable global average voltage, and globally coupled reactive power constraints.

The remainder of this paper is organized as follows. Section II presents the communication and the physical power network of the microgrid. The formulation of the proposed distributed optimization problem is presented in Section III and Section IV proposes a distributed primal-dual algorithm to solve the optimization problem. The performance of the proposed control approach is validated in Section V and finally conclusions are drawn in Section VI.

Notations: Define \mathbb{R}^N as the N dimensional real vector space and \mathbb{R}^N_+ as the nonnegative orthant in \mathbb{R}^N . Denote $\mathbf{0} \in \mathbb{R}^N$ as a column vector with all zeros and $\mathbf{1} \in \mathbb{R}^N$ as a column vector with all ones. For a vector $\mathbf{x} \in \mathbb{R}^N$, $\mathbf{x} \leq \mathbf{0}$ means each component of \mathbf{x} is less than or equal to zero. Denote $\mathrm{col}(\mathbf{x}_1,\cdots,\mathbf{x}_N)=(\mathbf{x}_1^\top,\cdots,\mathbf{x}_N^\top)^\top$ as the column vector stacked with column vectors $\mathbf{x}_1,\cdots,\mathbf{x}_N$. Given

a matrix $\mathbf{X} \in \mathbb{R}^{M \times N}$, we let $\mathbf{x}_{*,i}$ denote the *i*th column-vector of \mathbf{X} . For a set $\Omega \subset \mathbb{R}^N$, its relative interior is $\mathrm{rint}(\Omega)$. A projection operator is defined as $\mathcal{P}_C(\mathbf{z}) \triangleq \mathrm{argmin}_{\mathbf{x} \in C} \|\mathbf{x} - \mathbf{z}\|$.

II. MICROGRID AS A CYBER-PHYSICAL SYSTEM

A. Communication Network

Assume in an AC microgrid there are N dispatchable inverters, the set of which is denoted by $\mathcal{V}=\{1,2,\cdots,N\}$. The microgrid has a sparse communication network by which data is exchanged among the agents of the sources. The communication network is modeled as a directed graph $\mathcal{G}=\{\mathcal{V},\mathcal{E}\}$ in which the nodes are agents and the edges are the communication links connecting nodes. As in [4], [9], the communication links may exchange data with different gains and the edge weight between nodes i and j is $a_{ij}>0$. The communication graph can be represented by an adjacency matrix $\mathbf{A}=[a_{ij}]\in\mathbb{R}^{N\times N}$. Optimal design of the communication weights is out of the scope of this paper and can be found in [33]. Another matrix $\mathbf{A}'=[a'_{ij}]\in\mathbb{R}^{N\times N}$ that does not consider weights is defined as:

$$a'_{ij} = \begin{cases} 1, & a_{ij} \neq 0 \\ 0, & a_{ij} = 0. \end{cases}$$

A graph is said to have a spanning tree if it contains a root node from which there exists at least one direct path to every other node. The Laplacian matrix is defined as $\mathbf{L} = \mathbf{D}^{\mathrm{in}} - \mathbf{A}$ where $\mathbf{D}^{\mathrm{in}} = \mathrm{diag}\{d_i^{\mathrm{in}}\}$ is the in-degree matrix, $d_i^{\mathrm{in}} = \sum_{j \in \mathcal{N}_i} a_{ij}$, and \mathcal{N}_i is the set of the neighbors of node i. Similar to the indegree matrix, an out-degree matrix $\mathbf{D}^{\mathrm{out}} = \mathrm{diag}\{d_i^{\mathrm{out}}\}$ can also be defined with $d_i^{\mathrm{out}} = \sum_{j \in \mathcal{N}_i} a_{ji}$. The Laplacian matrix is balanced if the in-degree and out-degree matrices are equal.

B. Power Network

All the zero injection and load buses which are modeled as constant impedances are eliminated by Kron reduction, and only the buses at the outputs of the LC filters of the sources are kept. The corresponding reduced bus admittance matrix is denoted by \mathbf{Y} . In terms of network reduction in microgrids, both instantaneous and steady-state methods have been proposed in the literature [34]. Considering the instantaneous Kron reduction may result in a reduced network that does not present a physical circuit with passive elements, in this paper we apply the traditional Kron reduction in [35] that considers steady-state network parameters. Then the reactive power flow equations at bus i can be written as:

$$Q_i = v_i \sum_{j \in \mathcal{W}_i} v_j (G_{ij} \sin \theta_{ij} - B_{ij} \cos \theta_{ij}), \qquad (1)$$

where Q_i is the reactive power injection of inverter i, \mathcal{W}_i is the set of buses that connect with bus i (including bus i), v_i is the voltage magnitude of bus i in per unit, θ_i is the phase angle of bus i, $\theta_{ij} = \theta_i - \theta_j$, and G_{ij} and B_{ij} are the real and imaginary parts of the element in $\mathbf{Y} = \mathbf{G} + j\mathbf{B}$. Note that in the reduced network each bus is connected to all the other buses. The normalized reactive power for inverter i is:

$$\lambda_{Q_i} \stackrel{\triangle}{=} \frac{Q_i}{\overline{Q}_i},\tag{2}$$

3

where \overline{Q}_i is the upper limit of the reactive power for inverter i. Note that all values here are in per unit.

III. OPTIMIZATION PROBLEM FOR SECONDARY CONTROL

For frequency regulation, the same control as in [9] can be used. Here we focus on voltage and reactive power regulation in the secondary control. The design principles include:

- Distributed structure: The algorithm should be fully distributed and each agent updates its local variables only based on its local data and the information from its neighbors.
- 2) Optimality: The distributed algorithm to be developed should be guaranteed to converge to the same optimal solution as the original optimization problem for which a proper trade-off is made between voltage regulation and reactive power sharing among the DGs.
- 3) *Constraints*: The technical constraints on voltage magnitude and reactive power should always be satisfied.

A. Formulated Optimization Problem

The voltage and reactive power regulation in the secondary control is formulated as the following optimization problem:

$$\min_{\mathbf{v}} f(\mathbf{v}) = \sum_{i=1}^{N} f_i(\mathbf{v})$$
 (3a)

s.t.
$$\mathbf{1}^{\top}\mathbf{v}/N - v^{\mathrm{r}} = 0$$
 (3b)

$$-\lambda_{\mathbf{Q}}(\mathbf{v},\boldsymbol{\theta}) + \underline{\lambda}_{\mathbf{Q}} \le 0 \tag{3c}$$

$$\lambda_{\mathbf{Q}}(\mathbf{v}, \boldsymbol{\theta}) - \overline{\lambda}_{\mathbf{Q}} \le \mathbf{0}$$
 (3d)

$$-\mathbf{v} + \underline{\mathbf{v}} \le \mathbf{0},\tag{3e}$$

$$\mathbf{v} - \overline{\mathbf{v}} < \mathbf{0},\tag{3f}$$

where v^{r} is the rated voltage in per unit, $\mathbf{v} = [v_1, v_2, \cdots, v_N]^{\top}$ with lower and upper bounds as $\underline{\mathbf{v}} = [\underline{v}_1, \underline{v}_2, \cdots, \underline{v}_N]^{\top}$ and $\overline{\mathbf{v}} = [\overline{v}_1, \overline{v}_2, \cdots, \overline{v}_N]^{\top}$ (usually \underline{v}_i and \overline{v}_i are chosen as 0.95 and 1.05 respectively), $\boldsymbol{\theta} = [\theta_2, \cdots, \theta_N]^{\top}$ ($\theta_1 = 0$ is selected as the reference), $\boldsymbol{\lambda}_{\mathbf{Q}} = [\lambda_{Q_1}, \lambda_{Q_2}, \cdots, \lambda_{Q_N}]^{\top}$, and $\underline{\boldsymbol{\lambda}}_{\mathbf{Q}} = [\underline{\lambda}_{Q_1}, \underline{\lambda}_{Q_2}, \cdots, \underline{\lambda}_{Q_N}]^{\top}$ are the lower and upper limit vectors for normalized reactive power. The objective function for DG i, $f_i(\mathbf{v})$, is defined as:

$$f_i(\mathbf{v}) = \frac{\alpha |\mathcal{N}_i|^2}{2} \sigma_i^2 + \frac{\beta}{2} \sum_{j \in \mathcal{N}_i} a_{ij} (\lambda_{Q_i} - \lambda_{Q_j})^2$$

$$\stackrel{\triangle}{=} f_i^1(\mathbf{v}) + f_i^2(\mathbf{v}), \tag{4}$$

where

$$\sigma_i^2 = \sum_{j \in \mathcal{N}_i} \frac{\left(v_j - \sum_{k \in \mathcal{N}_i} v_k / |\mathcal{N}_i|\right)^2}{|\mathcal{N}_i|},\tag{5}$$

 $\alpha{\ge}0$ and $\beta{\ge}0$ ($\alpha\beta\neq0$) as design parameters, \mathcal{N}_i is the set of the in-neighbors of DG i in the communication network (including node i), and $|\mathcal{N}_i|$ is the cardinal number of \mathcal{N}_i . Note that the first term in (4) and the equality constraint in (3b) together will guarantee admissible voltage profiles while only one of them cannot. If α and β are chosen properly, the

voltage profile should be admissible for usual operating conditions. However, considering many different possible operating conditions it is still possible that the voltage magnitude of some DGs may violate their upper or lower bounds. For that reason, the constraints (3e)–(3f) are still needed.

B. Convex Optimization Problem

With the nonlinear reactive power injection functions in both objective function and inequality constraints, (3) is a nonlinear nonconvex optimization problem, which is very challenging to solve. In order to address this problem, we approximate the nonlinear reactive power injection functions and convert problem (3) to a convex optimization problem.

Specifically, it has been shown that the reactive power injection can be approximated as [36]:

$$\tilde{Q}_i = -\sum_{j=1}^{N} B_{ij} v_j - \sum_{j=1}^{N} G_{ij} \theta_j.$$
 (6)

It is clear that λ_{Q_i} is approximately a linear function of v_j for $j=1,\cdots,N$. As shown in both [36] and our own numerical experiments on AC microgrids, such an approximation has acceptable accuracy compared with the nonlinear reactive power injection in (1). Using $\tilde{\lambda}_{Q_i} = \tilde{Q}_i/\overline{Q}_i$ to approximate λ_{Q_i} , the objective function becomes:

$$\tilde{f}_{i}(\mathbf{v}) = \frac{\alpha |\mathcal{N}_{i}|^{2}}{2} \sigma_{i}^{2} + \frac{\beta}{2} \sum_{j \in \mathcal{N}_{i}} a_{ij} (\tilde{\lambda}_{Q_{i}} - \tilde{\lambda}_{Q_{j}})^{2}$$

$$\stackrel{\triangle}{=} f_{i}^{1}(\mathbf{v}) + \tilde{f}_{i}^{2}(\mathbf{v}). \tag{7}$$

Then the optimization problem (3) is modified to be:

$$\min_{\mathbf{v}} \tilde{f}(\mathbf{v}) = \sum_{i=1}^{N} \tilde{f}_i(\mathbf{v})$$
 (8a)

s.t.
$$\mathbf{1}^{\mathsf{T}}\mathbf{v}/N - v^{\mathsf{r}} = 0$$
 (8b)

$$-\tilde{\mathbf{B}}\mathbf{v} - \tilde{\mathbf{G}}\boldsymbol{\theta} + \underline{\boldsymbol{\lambda}}_{\mathbf{O}} \le \mathbf{0} \tag{8c}$$

$$\tilde{\mathbf{B}}\mathbf{v} + \tilde{\mathbf{G}}\boldsymbol{\theta} - \overline{\lambda}_{\mathbf{Q}} \le \mathbf{0}$$
 (8d)

$$-\mathbf{v} + \mathbf{v} < \mathbf{0} \tag{8e}$$

$$\mathbf{v} - \overline{\mathbf{v}} \le \mathbf{0},\tag{8f}$$

where the elements in $\tilde{\mathbf{B}}$ and $\tilde{\mathbf{G}}$ are obtained by $\tilde{B}_{ij} = -B_{ij}/\overline{Q}_i$ and $\tilde{G}_{ij} = -G_{ij}/\overline{Q}_i$.

 $-B_{ij}/\overline{Q}_i$ and $\tilde{G}_{ij} = -G_{ij}/\overline{Q}_i$. Let $h(\mathbf{v}) = \mathbf{1}^{\top} \mathbf{v}/N - v^r$. (8e)–(8f) are defined as local constraint set $\Omega_i = \{v_i \in \mathbb{R} | \underline{v}_i \leq v_i \leq \overline{v}_i\}$ for $i = 1, \dots, N$. The reactive power constraints (8c)–(8d) are denoted by $g(\mathbf{v}) \leq \mathbf{0}$

$$g(\mathbf{v}) \stackrel{\Delta}{=} \begin{bmatrix} g^{L}(\mathbf{v}) \\ g^{U}(\mathbf{v}) \end{bmatrix} = \begin{bmatrix} -\tilde{\mathbf{B}}\mathbf{v} - \tilde{\mathbf{G}}\boldsymbol{\theta} + \underline{\boldsymbol{\lambda}}_{\mathbf{Q}} \\ \tilde{\mathbf{B}}\mathbf{v} + \tilde{\mathbf{G}}\boldsymbol{\theta} - \overline{\boldsymbol{\lambda}}_{\mathbf{Q}} \end{bmatrix}. \tag{9}$$

Then the optimization problem (8) is equivalently written as:

$$\min_{\mathbf{v} \in \Omega} \tilde{f}(\mathbf{v}) = \sum_{i=1}^{N} \tilde{f}_i(\mathbf{v})$$
 (10a)

$$s.t. h(\mathbf{v}) = 0 (10b)$$

$$\mathbf{g}(\mathbf{v}) < \mathbf{0},\tag{10c}$$

where $\Omega \triangleq \prod_{i \in \mathcal{V}} \Omega_i \subset \mathbb{R}^N$ denotes the local constraints of the N agents and its relative interior is $\operatorname{rint}(\Omega)$.

C. Convexity of Problem (10)

Note that

$$\frac{\partial f_i^1(\mathbf{v})}{\partial v_i} = \alpha \sum_{j \in \mathcal{N}_i} (v_i - v_j). \tag{11}$$

Similarly the partial derivatives of f_i^1 with respect to v_j $(j \in \mathcal{N}_i)$ and v_k $(k \notin \mathcal{N}_i)$ can be obtained as:

$$\frac{\partial f_i^1(\mathbf{v})}{\partial v_j} = \alpha \sum_{k \in \mathcal{N}_i} (v_j - v_k) \text{ and } \frac{\partial f_i^1(\mathbf{v})}{\partial v_k} = 0.$$

The partial derivative of \tilde{f}_i with respect to v_i is:

$$\frac{\partial \tilde{f}_{i}(\mathbf{v})}{\partial v_{i}} = \sum_{j \in \mathcal{N}_{i}} \left(\alpha(v_{i} - v_{j}) + \beta a_{ij} (\tilde{\lambda}_{Q_{i}} - \tilde{\lambda}_{Q_{j}}) \frac{\partial (\tilde{\lambda}_{Q_{i}} - \tilde{\lambda}_{Q_{j}})}{\partial v_{i}} \right), (12)$$

where

$$\frac{\partial(\tilde{\lambda}_{Q_i} - \tilde{\lambda}_{Q_j})}{\partial v_i} = \frac{-B_{ii}}{\overline{Q}_i} + \frac{B_{ij}}{\overline{Q}_j} \triangleq d_i.$$
 (13)

It is clear that f_i^1 is a convex function of \mathbf{v} . To check the convexity of \tilde{f}_i with respect to \mathbf{v} we only need to check the convexity of $F_{ij} = (\tilde{\lambda}_{Q_i} - \tilde{\lambda}_{Q_j})^2/2$ for $j \in \mathcal{N}_i$. For $j \in \mathcal{N}_i$ we have

$$\frac{\partial (\tilde{\lambda}_{Q_i} - \tilde{\lambda}_{Q_j})}{\partial v_j} = \frac{-B_{ij}}{\overline{Q}_i} + \frac{B_{jj}}{\overline{Q}_j} \triangleq d_j.$$

For $k \neq i, j \in \mathcal{N}_i$, we have

$$\frac{\partial (\tilde{\lambda}_{Q_i} - \tilde{\lambda}_{Q_j})}{\partial v_k} = \frac{-B_{ik}}{\overline{Q}_i} + \frac{B_{jk}}{\overline{Q}_j} \triangleq d_k.$$

Then there is

$$\frac{\partial^2 F_{ij}}{\partial v_l v_m} = d_l d_m, \ l, m \in \{i, j, k\}. \tag{14}$$

Let $\mathbf{d} = [d_1, d_2, \cdots, d_N]^{\top}$, the Hessian matrix for F_{ij} with respect to \mathbf{v} can be written as

$$\nabla^2 F_{ij} = \mathbf{dd}^{\top}. \tag{15}$$

For all z, since

$$\mathbf{z}^{\mathsf{T}} \nabla^2 F_{ij} \mathbf{z} = \mathbf{z}^{\mathsf{T}} \mathbf{d} \mathbf{d}^{\mathsf{T}} \mathbf{z} = (\mathbf{z}^{\mathsf{T}} \mathbf{d})^2 \ge 0,$$
 (16)

 $\nabla^2 F_{ij}$ is positive semidefinite, indicating that F_{ij} is a convex function of \mathbf{v} and further \tilde{f}_i is a convex function of \mathbf{v} since nonnegative weighted sums preserve convexity. Therefore, problem (10) is a convex optimization problem.

D. Distinct Features of the Proposed Formulation

Different from most distributed optimization based voltage control methods developed for grid-following inverters, such as in [31], the proposed formulation is for grid-forming inverters for which the control variables are voltage instead of reactive power injection.

4

- 2) The proposed formulation is more general than existing methods and makes possible a proper trade-off between voltage regulation and reactive power-sharing and also obeying constraints on both voltage magnitude and reactive power of all sources. Typical existing methods can be considered as special cases of the proposed formulation. For example, the droop-free control in [9] can be obtained by setting α to be zero and removing all inequality constraints.
- 3) Voltage regulation objective is achieved by the first term in the objective function for voltage variance, the equality constraint for average voltage, and the inequality constraints (8e)–(8f). If there is only the average voltage equality constraint, it is not possible to guarantee that the voltage profile is good and the voltage deviation will be within ±5% of the rated voltage, as shown in [3].
- 4) The voltage control problem is explicitly formulated as an optimization problem for which distributed algorithms can be developed by adapting the standard methods such as primal-dual gradient algorithm to theoretically guarantee convergence and optimality. This is distinct from most existing methods such as in [3], [9] in which PI controllers are extensively used.
- 5) By utilizing the linearized reactive power injection function, the proposed optimization problem has been mathematically proven to be a convex optimization problem which makes possible an efficient and reliable algorithm for solving such a problem.

IV. PRIMAL-DUAL GRADIENT BASED DISTRIBUTED SOLVING ALGORITHM

In order to solve problem (10), we develop a distributed algorithm based on the primal-dual gradient algorithm by addressing some unique challenges. The following assumptions are needed to ensure the well-posedness of problem (10) [37].

Assumption 1.

- 1) (Convexity and continuity) For $i \in V$, Ω_i is compact and convex. On an open set containing Ω_i , \tilde{f}_i is strictly convex, h and g are convex, and \tilde{f}_i , h, and g are locally Lipschitz continuous.
- 2) (Slater's constraint qualification) There exists $\check{\mathbf{v}} \in \operatorname{rint}(\Omega)$ such that $h(\check{\mathbf{v}}) = 0$ and $g(\check{\mathbf{v}}) < \mathbf{0}$.
- (Communication topology) The communication network G has a spanning tree and a balanced Laplacian matrix.

These assumptions are quite mild and similar ones are widely used in the literature, such as [3], [4], [9], [37], [38].

Remark. Although Condition 3 in Assumption 1 only requires a directed communication network that has a spanning tree and a balanced Laplacian matrix to make the proposed control

to work, in this paper in the practical implementation we require the communication network to be undirected in addition to satisfying Condition 3. Then when there are communication link (bi-directional) losses, as long as the communication network still has a spanning tree it will still have a balanced Laplacian matrix so that Condition 3 is still satisfied, which will significantly enhance the resiliency of the proposed control algorithm against potential communication link losses compared with the case with a directed communication network.

A. Augmented Lagrangian

We introduce Lagrangian multipliers μ for the equality constraint (10b), and $\boldsymbol{\xi} = \operatorname{col}(\underline{\boldsymbol{\xi}}, \overline{\boldsymbol{\xi}})$ with $\underline{\boldsymbol{\xi}} = [\underline{\xi}_1, \cdots, \underline{\xi}_N]^{\top}$ and $\overline{\boldsymbol{\xi}} = [\overline{\xi}_1, \cdots, \overline{\xi}_N]^{\top}$ for the reactive power inequality constraints $\boldsymbol{g}^{\mathrm{L}} \leq \boldsymbol{0}$ and $\boldsymbol{g}^{\mathrm{U}} \leq \boldsymbol{0}$. For the optimization problem in (10), the augmented Lagrangian is defined as [39], [40]:

$$L(\hat{\mathbf{v}}, \mu, \boldsymbol{\xi}) \triangleq \tilde{f}(\hat{\mathbf{v}}) + \mu |h(\hat{\mathbf{v}})| + \boldsymbol{\xi}^{\mathsf{T}} \boldsymbol{g}^{\mathsf{L}}(\hat{\mathbf{v}}) + \overline{\boldsymbol{\xi}}^{\mathsf{T}} \boldsymbol{g}^{\mathsf{U}}(\hat{\mathbf{v}}). \quad (17)$$

Augmented Lagrangian instead of the standard Lagrangian is used because the primal-dual gradient algorithm associated with the augmented Lagrangian has better convergence properties [31]. The equality constraints are treated in a similar way as in [40] in which a penalty function is defined.

B. Standard Primal-Dual Gradient Algorithm

The standard primal-dual gradient algorithm [31], [37], [41] for solving (8) can be written as:

$$\hat{v}_{i}[n+1] = \mathcal{P}_{\Omega_{i}}\left(\hat{v}_{i}[n] - \tau \frac{\partial L(\hat{\mathbf{v}}[n], \mu[n], \boldsymbol{\xi}[n])}{\partial v_{i}}\right)$$

$$= \mathcal{P}_{\Omega_{i}}\left(\hat{v}_{i}[n] - \tau \left(\sum_{j=1}^{N} \frac{\partial \tilde{f}_{j}(\hat{\mathbf{v}}[n])}{\partial v_{i}}\right)\right)$$

$$+ \mu[n]\mathcal{D}_{v_{i}}|h(\hat{\mathbf{v}}[n])| + \sum_{j=1}^{N} \tilde{B}_{ji}(\overline{\xi}_{j}[n] - \underline{\xi}_{j}[n])\right)$$

$$\mu[n+1] = \mu[n] + \gamma \frac{\partial L(\hat{\mathbf{v}}[n], \mu[n], \boldsymbol{\xi}[n])}{\partial \mu}$$

$$= \mu[n] + \gamma|h(\hat{\mathbf{v}}[n])| \qquad (19)$$

$$\underline{\xi}_{i}[n+1] = \mathcal{P}_{\mathbb{R}_{+}}\left(\underline{\xi}_{i}[n] + \varphi \frac{\partial L(\hat{\mathbf{v}}[n], \mu[n], \boldsymbol{\xi}[n])}{\partial \underline{\xi}_{i}}\right)$$

$$= \mathcal{P}_{\mathbb{R}_{+}}\left(\underline{\xi}_{i}[n] + \varphi \frac{\partial L(\hat{\mathbf{v}}[n], \mu[n], \boldsymbol{\xi}[n])}{\partial \overline{\xi}_{i}}\right)$$

$$\overline{\xi}_{i}[n+1] = \mathcal{P}_{\mathbb{R}_{+}}\left(\overline{\xi}_{i}[n] + \varphi \frac{\partial L(\hat{\mathbf{v}}[n], \mu[n], \boldsymbol{\xi}[n])}{\partial \overline{\xi}_{i}}\right)$$

where \mathcal{D}_{v_i} is the operator for subgradient with respect to v_i , g_i^{L} (g_i^{U}) is the ith element of \mathbf{g}^{L} (\mathbf{g}^{U}), and τ , γ , and φ are positive scalar design parameters. Here $\hat{v}_i[n]$ is the voltage set point decided by the primal-dual gradient algorithm at time step n. Since the zero-level control of inverter i will track $\hat{v}_i[n]$ and control the output voltage $v_i[n]$ to be $\hat{v}_i[n]$, in the following sections the actual measured values $v_i[n]$ instead of $\hat{v}_i[n]$ will be used for the update.

(21)

 $= \mathcal{P}_{\mathbb{R}_+} \Big(\overline{\xi}_i[n] + \varphi \, g_i^{\mathrm{U}}(\hat{\mathbf{v}}[n]) \Big),$

However, there are the following major challenges for implementing the primal-dual gradient algorithm in an efficient, distributed manner, which we will address separately.

- 1) Non-separable objective function: The objective function in (10) is $\tilde{f} = \sum_{j=1}^{N} \tilde{f}_{j}(\mathbf{v})$ in which $\tilde{f}_{j}(\mathbf{v})$ is a function of \mathbf{v} instead of only a function of v_{j} . Therefore, when calculating $\partial \tilde{f}/\partial v_{i}$ in (18), the terms $\partial \tilde{f}_{j}/\partial v_{i}$ for $j \notin \mathcal{N}_{i}$ is not available for agent i, and thus (18) is not fully distributed.
- 2) Unavailable global average voltage: For the μ update in (19), the global average voltage is needed but is not available for each agent.
- 3) Globally coupled reactive power constraints: The reactive power injection in the reduced network is a function of all v_i 's. Consequently, (18) needs information of the whole ξ and (20)–(21) need information of the whole \mathbf{v} , which, however, are not available for each agent.

The last three challenges will be discussed and addressed in more detail in Sections IV-C-IV-E below.

C. Non-Separable Objective Function

For agent i, the objective function $\tilde{f}(\mathbf{v})$ can be approximated around $v_i[n]$ as [42]:

$$\tilde{f}(\mathbf{v}) = \tilde{f}_i(\mathbf{v}) + \pi_i[n](v_i - v_i[n]), \tag{22}$$

where $\pi_i[n]$ is the partial derivative of $\sum_{j\neq i} \tilde{f}_j(\mathbf{v})$ with respect to v_i at $v_i[n]$:

$$\pi_i[n] \triangleq \sum_{j \neq i} \frac{\partial \tilde{f}_j(\mathbf{v}[n])}{\partial v_i}.$$
 (23)

Note that the evaluation of $\pi_i[n]$ requires all $\partial \tilde{f}_j(\mathbf{v}[n])/\partial v_i$ which may not be available locally at node i. To solve this problem, consider [42]:

$$\pi_{i}[n] = N \underbrace{\left(\frac{1}{N} \sum_{j=1}^{N} \frac{\partial \tilde{f}_{j}(\mathbf{v}[n])}{\partial v_{i}}\right)}_{D_{i}[n]} - \frac{\partial \tilde{f}_{i}(\mathbf{v}[n])}{\partial v_{i}}, \qquad (24)$$

where $D_i[n]$ can be estimated by a distributed observer based on dynamic consensus [4], [9], [43] as:

$$\hat{D}_{i}^{j}[n] = \frac{\partial \tilde{f}_{j}(\mathbf{v}[n])}{\partial v_{i}} + \sum_{t=0}^{n} \sum_{k \in \mathcal{N}_{j}} a_{jk} \left(\hat{D}_{i}^{k}[t] - \hat{D}_{i}^{j}[t] \right) \Delta t,$$

$$j = 1, \dots, N, \qquad (25)$$

where \hat{D}_i^j is the estimate of D_i by DG j and Δt is the step size. Note that \hat{D}_i^j will converge to the true average if the communication network has a spanning tree and a balanced Laplacian matrix [4], [37]. Detailed mathematical analysis can be found in Appendix. Then $\pi_i[n]$ is replaced by $\tilde{\pi}_i[n]$ as:

$$\tilde{\pi}_i[n] = N\hat{D}_i^i[n] - \frac{\partial \tilde{f}_i(\mathbf{v}[n])}{\partial v_i}.$$
 (26)

(33)

D. Distributed Average Voltage Estimation

In $h(\mathbf{v}) = \mathbf{1}^{\top} \mathbf{v}/N - v^{\mathrm{r}}$, the average voltage of all inverter output buses, $(\mathbf{1}^{\top}\mathbf{v}[n]/N)$, can be estimated by agent i = $1, \ldots, N$ as $v_i^{\text{av}}[n]$ using the following distributed observer based on dynamic consensus [4], [9]:

$$v_i^{\text{av}}[n] = v_i[n] + \sum_{t=0}^n \sum_{j \in \mathcal{N}_i} a_{ij} (v_j^{\text{av}}[t] - v_i^{\text{av}}[t]) \Delta t,$$
 (27)

where Δt is the step size. It has been proven in [4] that for $\forall i = 1, 2, \dots, N, v_i^{\text{av}}$ converges to a consensus value which is the true global average voltage when the communication network has a spanning tree and a balanced Laplacian matrix.

Since each agent will have its own estimate of $h(\mathbf{v})$, it will have its own μ . We denote the μ for agent i by μ_i . With v_i^{av} converging to the true global average voltage, from (19) it is clear that the μ_i 's will achieve a consensus.

E. Coupled Reactive Power Inequality Constraints

In (18), the term related to the reactive power inequality constraints (10c) is $\sum_{j=1}^{N} \tilde{B}_{ji}(\overline{\xi}_{j} - \underline{\xi}_{j})$. It is clear that it depends on $\overline{\xi}_j$ and $\underline{\xi}_i$ for all agents, mainly because the reactive power inequality constraints are coupled. This will make the distributed implementation very challenging.

In order to address this problem, we write the coupled inequality constraints as $g(\mathbf{v}) \triangleq \sum_{i \in \mathcal{V}} g_i(v_i) \leq \mathbf{0}$, where $\boldsymbol{g}_i:\Omega_i \to \mathbb{R}^{2N}$ can be written as

$$\boldsymbol{g}_{i}(v_{i}) = \frac{\left[\boldsymbol{g}_{i}^{\mathrm{L}}(v_{i})\right]}{\left[\boldsymbol{g}_{i}^{\mathrm{U}}(v_{i})\right]} = \begin{bmatrix} -\tilde{B}_{1i}v_{i} - \tilde{G}_{1i}\theta_{i} + a'_{1i}\underline{\lambda}'_{Q_{1}} \\ \vdots \\ -\tilde{B}_{Ni}v_{i} - \tilde{G}_{Ni}\theta_{i} + a'_{Ni}\underline{\lambda}'_{Q_{N}} \\ \tilde{B}_{1i}v_{i} + \tilde{G}_{1i}\theta_{i} - a'_{1i}\overline{\lambda}'_{Q_{1}} \\ \vdots \\ \tilde{B}_{Ni}v_{i} + \tilde{G}_{Ni}\theta_{i} - a'_{Ni}\overline{\lambda}'_{Q_{N}} \end{bmatrix}, (28)$$

where θ_i can be obtained locally by the installed phasor measurement unit (PMU) and for j = 1, ..., N there are

$$\underline{\lambda}'_{Q_j} = \left\{ \begin{array}{ll} \frac{\lambda_{Q_j}}{|\mathcal{N}_j|}, & \text{if } a'_{ji} \neq 0 \\ 1, & \text{otherwise} \end{array} \right. \text{ and } \overline{\lambda}'_{Q_j} = \left\{ \begin{array}{ll} \frac{\overline{\lambda}_{Q_j}}{|\mathcal{N}_j|}, & \text{if } a'_{ji} \neq 0 \\ 1, & \text{otherwise}. \end{array} \right.$$

Note that for every $i \in \mathcal{V}$ agent i only has access to $g_i(v_i)$ in (28) rather than $g(\mathbf{v})$, and $g_i(v_i)$ only depends on the data of agent i and the information from its neighbors.

To achieve the actual constraint of (9) based on the local $g_i(v_i)$ in (28), the dynamic consensus method can be used. Specifically, the average $\sum_{i=1}^{N} g_i(v_i)/N$ can be estimated as:

$$\boldsymbol{g}_{i}^{\text{av}}[n] = \boldsymbol{g}_{i}(v_{i}[n]) + \sum_{t=0}^{n} \sum_{j \in \mathcal{N}_{i}} a_{ij} (\boldsymbol{g}_{j}^{\text{av}}[t] - \boldsymbol{g}_{i}^{\text{av}}[t]) \Delta t, \quad (29)$$

where $g_i^{av}[n]$ is the average value estimated by DG i. Thus $m{g}(\mathbf{v}[n])$ can be obtained as $Nm{g}_i^{\mathrm{av}}[n].$ Then for agent i we replace $g(\mathbf{v}[n])$ by $\tilde{g}_i[n]$ as:

$$\tilde{\boldsymbol{g}}_{i}[n] \stackrel{\triangle}{=} \frac{\left[\tilde{\boldsymbol{g}}_{i}^{\mathrm{L}}[n]\right]}{\left[\tilde{\boldsymbol{g}}_{i}^{\mathrm{U}}[n]\right]} = N\boldsymbol{g}_{i}^{\mathrm{av}}[n]. \tag{30}$$

F. Proposed Algorithm

Based on the above discussion, in order to solve the problem in (10) fully distributedly we construct a modified Lagrangian function for the problem in (10) as:

$$\tilde{L}(\mathbf{v}, \mu, \boldsymbol{\xi}) \triangleq \tilde{f}(\mathbf{v}) + \mu |h(\mathbf{v})| + \underline{\boldsymbol{\xi}}^{\top} \sum_{i \in \mathcal{V}} \boldsymbol{g}_{i}^{\mathrm{L}}(v_{i}) + \overline{\boldsymbol{\xi}}^{\top} \sum_{i \in \mathcal{V}} \boldsymbol{g}_{i}^{\mathrm{U}}(v_{i}).$$

Different from (20)–(21) in which agent i only updates the Lagrangian multiplier ξ_i for its own reactive power inequality constraint, here we let agent i maintain a collection of local multipliers $\boldsymbol{\xi}_i \triangleq \operatorname{col}(\underline{\boldsymbol{\xi}}_i, \overline{\boldsymbol{\xi}}_i) \in \mathbb{R}^{2N}$ for all reactive power inequality constraints. We develop the following primal-dual gradient based algorithm utilizing the techniques in Sections IV-C-IV-E. For agent i, it can be written as:

$$\hat{v}_{i}[n+1] = \mathcal{P}_{\Omega_{i}} \left(v_{i}[n] - \tau \frac{\partial \hat{L}(\mathbf{v}[n], \mu_{i}[n], \boldsymbol{\xi}_{i}[n])}{\partial v_{i}} \right) \\
= \mathcal{P}_{\Omega_{i}} \left(v_{i}[n] - \tau \left(N \hat{D}_{i}^{i}[n] \right) \right) \\
+ \mu_{i}[n] \mathcal{D}_{v_{i}} | v_{i}^{\text{av}}[n] - v^{\text{r}}| + \tilde{\mathbf{b}}_{*,i}^{\mathsf{T}} (\overline{\boldsymbol{\xi}}_{i}[n] - \underline{\boldsymbol{\xi}}_{i}[n]) \right) \right) (31)$$

$$\mu_{i}[n+1] = \mu_{i}[n] + \gamma \frac{\partial \tilde{L}(\mathbf{v}[n], \mu_{i}[n], \boldsymbol{\xi}_{i}[n])}{\partial \mu} \\
= \mu_{i}[n] + \gamma | v_{i}^{\text{av}}[n] - v^{\text{r}}| (32)$$

$$\underline{\boldsymbol{\xi}}_{i}[n+1] = \mathcal{P}_{\mathbb{R}_{+}^{N}} \left(\underline{\boldsymbol{\xi}}_{i}[n] + \varphi \nabla_{\underline{\boldsymbol{\xi}}} \tilde{L}(\mathbf{v}[n], \mu_{i}[n], \boldsymbol{\xi}_{i}[n]) \right) \\
= \mathcal{P}_{\mathbb{R}_{-}^{N}} \left(\boldsymbol{\xi}_{i}[n] + \varphi \tilde{\boldsymbol{g}}_{i}^{\mathbf{L}}[n] \right) (33)$$

$$\overline{\boldsymbol{\xi}}_{i}[n+1] = \mathcal{P}_{\mathbb{R}_{+}^{N}} \left(\overline{\boldsymbol{\xi}}_{i}[n] + \varphi \nabla_{\overline{\boldsymbol{\xi}}} \tilde{L}(\mathbf{v}[n], \mu_{i}[n], \boldsymbol{\xi}_{i}[n]) \right)
= \mathcal{P}_{\mathbb{R}_{+}^{N}} \left(\overline{\boldsymbol{\xi}}_{i}[n] + \varphi \, \tilde{\boldsymbol{g}}_{i}^{\mathrm{U}}[n] \right),$$
(34)

where $\hat{\mathbf{b}}_{*,i}$ is the *i*th column vector of the $\tilde{\mathbf{B}}$ matrix. Then, each agent i commits its own optimization variable by setting the voltage magnitude reference for inverter i, $v_i^{\text{ref}}[n+1]$, to be $\hat{v}_i[n+1]$. The zero-level control of inverter i will track this reference and control the output voltage $v_i[n+1]$ to be $\hat{v}_i[n+1]$, and $v_i[n+1]$ will be used for the next time step. Note that in the proposed algorithm the number of DGs N is needed, which may not be known to each DG. One potential approach is to distributedly estimate it such as by a distributed L2-norm estimation method based on dynamic average consensus [44].

The parameters τ , γ , and φ impact the convergence of the proposed algorithm. Too large values may affect the stability while too small values may make the convergence very slow. In [30] a theoretical upper bound is presented for similar parameters, which, however, are conservative. In [30] these parameters actually still need to be selected using some trial and error methods. Similar to [30] we have also selected these parameters based on some numerical simulations and testing to guarantee acceptable convergence performance.

The proposed algorithm is presented as Algorithm 1. The information flow of the proposed control is shown in Fig. 1. Different from [37] for which there are only inequality constraints, in (10) there is a coupled equality constraint which requires global information about the average voltage of the

ALGORITHM 1 Distributed solving algorithm

Initialization: Set $v_i[0] = v_i^{\text{meas}}, \ \mu_i[0] = 0, \ \boldsymbol{\xi}_i[0] = \boldsymbol{0}, \ v_i^{\text{av}}[0] = v_i[0], \ \hat{D}_i^i[0] = \partial \tilde{f}_i(\mathbf{v}[0])/\partial v_i, \ \boldsymbol{g}_i^{\text{av}}[0] = \boldsymbol{g}_i(v_i[0]), \ \tilde{\boldsymbol{g}}_i[0] = N\boldsymbol{g}_i^{\text{av}}[0] \ \text{for} \ \forall i=1,\dots,N. \ \text{Set} \ n=0.$

(S.1) Each agent i updates its variables $\hat{v}_i[n+1]$, $\mu_i[n+1]$, $\boldsymbol{\xi}_i[n+1]$, and $\overline{\boldsymbol{\xi}}_i[n+1]$ based on (31)–(34);

(§.2) Each agent i sets voltage magnitude reference for inverter i as $v_i^{\text{ref}} = \hat{v}_i[n+1]$ and send it to zero-level control which controls the voltage $v_i[n+1]$ to v_i^{ref} ;

(S.3) Each agent i updates $\hat{D}_i^i[n]$ and $\tilde{\pi}_i[n]$ based on (25)–(26):

(S.4) Each agent i updates $\boldsymbol{g}_{i}^{\mathrm{av}}[n]$ and $\tilde{\boldsymbol{g}}_{i}[n]$ based on (29)–(30);

(S.5) Increase n by 1 and go to (S.1)

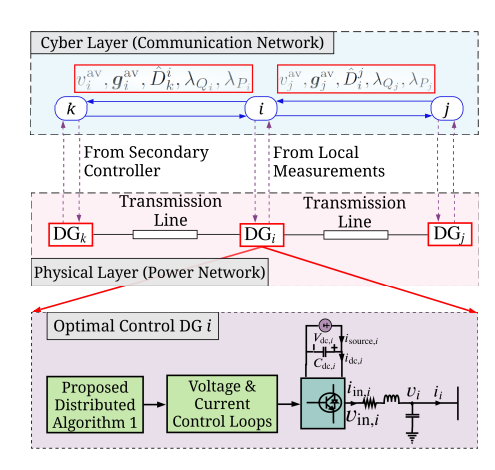


Fig. 1. Information flow in the proposed control.

system. First, the method in Section IV-D is needed to obtain the global information in a distributed manner. Second, in the proposed algorithm both coupled inequality constraints and coupled equality constraint are considered. Third, the proposed algorithm uses a dynamic consensus based approach to deal with the coupled inequality constraints, which is different from the nonsmooth penalty function based approach in [37].

The parameters in $\tilde{\mathbf{G}}$ and $\tilde{\mathbf{B}}$ (\tilde{G}_{ki} and \tilde{B}_{ki} for k = 1, ..., N) and \tilde{B}_{jk} for $j \in \mathcal{N}_i, k = 1, ..., N$) are assumed to be known to DG i. If they are not known, they can be estimated distributedly by adapting the ADMM based distributed robust estimation method in [45] or the data driven parameter estimation method presented in [46].

V. RESULTS

The performance of the proposed optimal distributed control is evaluated through simulations on the 4-DG microgrid test system in [3] shown in Fig. 2 and the modified IEEE 34-bus distribution test system shown in Fig. 3. Real-time simulations for the 4-DG system are performed on OPAL-RT OP4510 at 50 μs fixed time step using the ODE-5 (Dormand-Prince) solver. Real-time simulators help perform dynamic simulations efficiently and thus enable us to observe the detailed controller performances when both Q-V and $P-\omega$ loops run simultaneously. The updates of the distributed algorithm

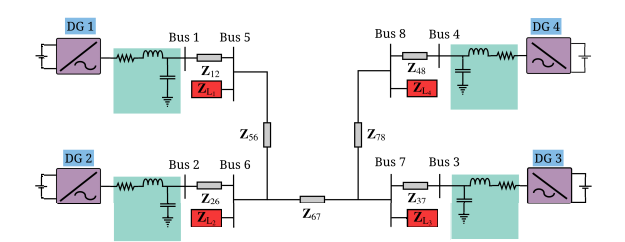


Fig. 2. Schematic diagram of the 4-DG test network.

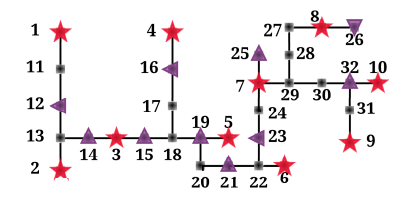


Fig. 3. Modified IEEE 34-bus distribution test system. The stars indicate DGs and the triangles indicate loads.

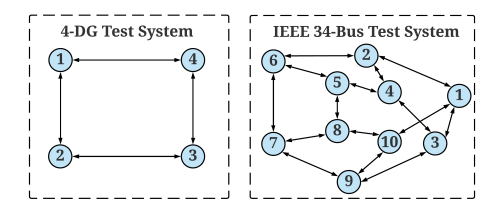


Fig. 4. Communication networks of the 4-DG test system and the IEEE 34-bus test system.

are also performed at 50 µs time step and we consider only a single consensus iteration at each time step. We use the 2-level power electronic switching model for the inverters [47]. The switching frequencies of the PWM generators are considered as 16200 Hz. To damp out the undesired low-frequency harmonics the cut-off frequencies of the measurement filters are selected as low as 3 Hz.

For the IEEE 34-bus test system, we have implemented the proposed control and the control in [9] in Matlab without detailed zero-level control loops. The Matlab simulations are performed as phasor simulation without consideration of detailed electromagnetic transients of the system [48].

A. Parameters Setup

The parameters τ , γ , and φ are selected as 0.0005, 0.005, and 0.01. Different values of α and β are used for different cases to provide flexibility. The reactive power limits are selected as $\underline{\lambda}_{Q_i}=0.2$ and $\overline{\lambda}_{Q_i}=0.8$ for all DGs. \underline{v}_i and \overline{v}_i for all DGs are chosen as 0.95 and 1.05. The communication networks used for the 4-DG test system and the IEEE 34-bus test systems are shown in Fig. 4 which both satisfy the condition 3 in Assumption 1. For the nonzero elements in \mathbf{A} we choose $a_{ij}=0.25$ for the 4-DG system and $a_{ij}=0.0625$ for the IEEE 34-bus system based on our numerical tests.

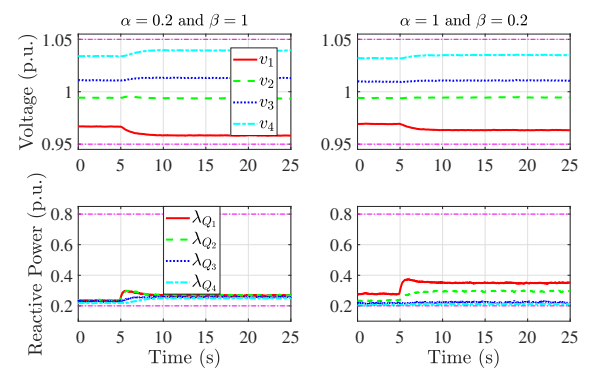


Fig. 5. Performance evaluation of the proposed control under different α and β . Load change is applied at 5 s.

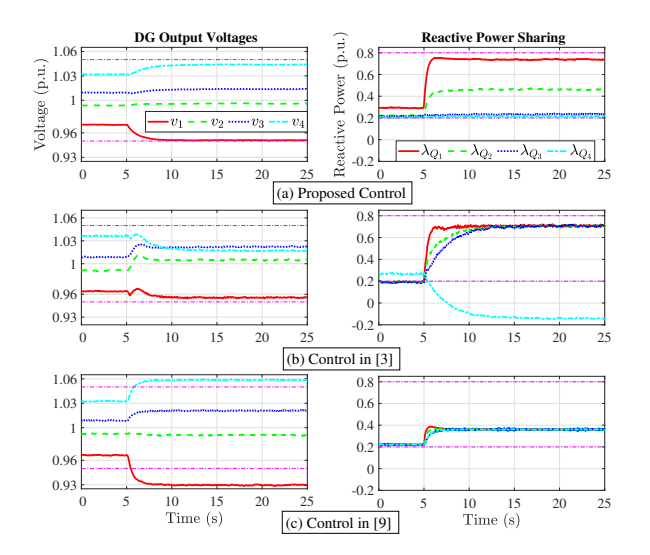


Fig. 6. Comparison between the proposed control and the controls in [3] and [9]. Load change is applied at 5 s.

B. 4-DG System

Real-time simulations on OPAL-RT OP4510 are performed for a 4-DG islanded microgrid test system as shown in Fig. 2. The parameters of this system are adopted from [3]. For the implementation of the proposed algorithm we have used DG output voltage and phase angle measurements from Simulink measurement blocks. The $(\tilde{\lambda}_{Q_i} - \tilde{\lambda}_{Q_j})$ term in (12) is replaced by $(\lambda_{Q_i} - \lambda_{Q_j})$ which can be obtained from the Simulink reactive power measurement blocks.

- 1) Performance under different α and β : The controller performance under normal loading conditions with different α and β are demonstrated in Fig. 5. The uniqueness of the proposed control is that it allows flexibility in coordinating voltage regulation and reactive power sharing by adjusting these two parameters. From the left-hand side of Fig. 5 it can be seen that the controller can almost achieve proportional reactive power sharing with small α . When α is increased, the voltage bounds become tighter at the cost of increased deviations in reactive power sharing which is clear from the right-hand side subfigures of Fig. 5.
- 2) Performance under heavy load scenario: The distributed control in [3] guarantees admissible voltage profile at the cost of relaxed reactive power sharing for one special DG

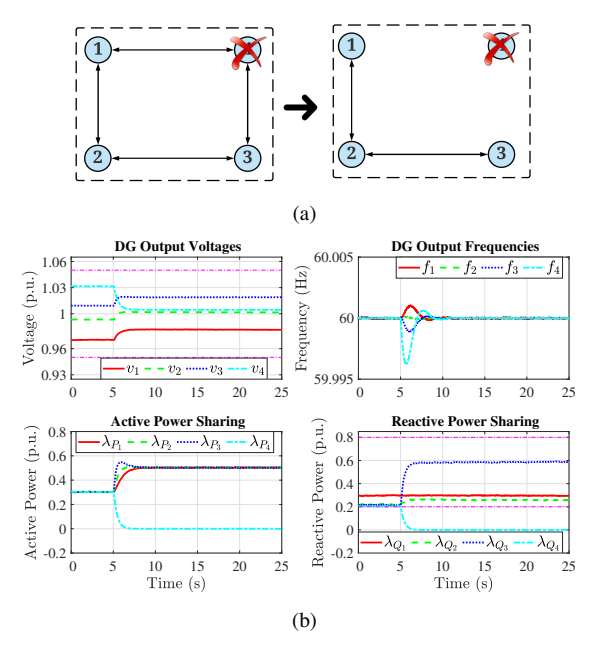


Fig. 7. Controller performance when source 4 is disconnected at 5 s. (a) Communication network after source 4 disconnection and (b) Controller performance.

and the control in [9] achieves proportional reactive power sharing without imposing bounds on voltages. By contrast, the proposed optimal control achieves a trade-off between voltage regulation and reactive power sharing objectives. In Fig. 6, we have considered an extreme scenario where at 5 s a large load is connected to the bus close to DG1. α and β are chosen as 1 and 0.065, respectively. For the proposed control, the voltages range between 0.95 and 1.042, while for the control in [3] the voltages range between 0.927–1.06 which violates the IEEE standard acceptable limits (0.95–1.05). In the case of reactive power sharing, the reactive power under proposed control ranges between 0.218 and 0.738 whereas for the control in [3] it ranges between -0.165 and 0.747.

- 3) Performance under source loss: Plug and play is an important feature of a microgrid system. The microgrid needs to accommodate the disconnection/addition of a source/load. Fig. 7 shows the performance of the proposed control when source 4 is intentionally unplugged at 5 s. Due to the disconnection of this source, the communication links connected to DG4 becomes unavailable. The proposed control can still work well as long as the communication network remains connected and balanced [3], [9]. After the disconnection, the active and reactive power injection from the DG4 goes to zero. It is seen that the proposed control effectively coordinates the voltage regulation and reactive power sharing of the remaining DGs and also guarantees that the constraints on reactive power and voltage are satisfied for the remaining DGs.
- 4) Performance under communication link loss: The performance of the proposed distributed control is validated under communication link loss. In Fig. 8 the communication link between the DGs 3 and 4 is disconnected at 5 s. Despite the loss of this communication link the communication network remains connected and has a balanced Laplacian matrix. At

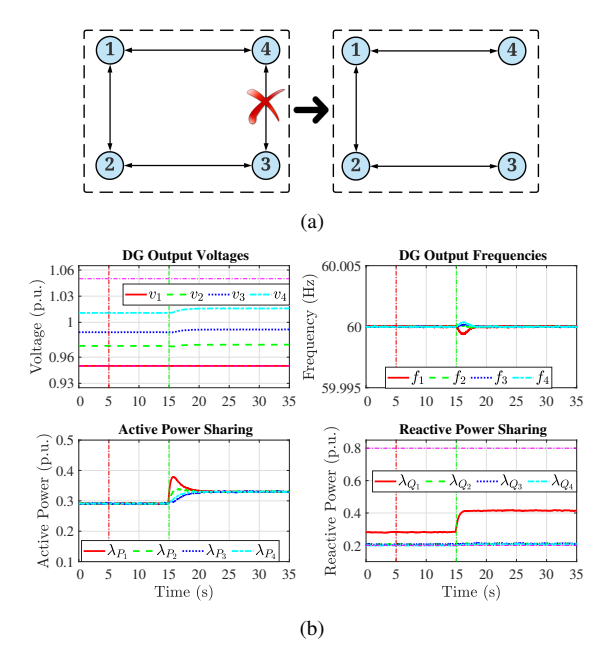


Fig. 8. Controller performance when communication link 3–4 is disconnected at 5 s. Load change is applied at 15 s. (a) Communication network after the link loss and (b) Controller performance.

- 15 s we apply a load change to demonstrate the controller performance under the considered communication link loss. It is seen that the proposed control can still work properly.
- 5) Performance under communication delay: The performance of the proposed control is validated under different communication delays. In Fig. 9 the communication delays are activated at 5 s and a load change is applied at 25 s. Due to the communication delay the most updated values are unavailable and the controller only utilizes the available last data point. From Fig. 9 it is seen that with the increase of communication delay the controller performance deteriorates and the oscillation increases, but with 9-ms of communication delay the performance is still acceptable and both voltage and reactive power can still stabilize.

C. IEEE 34-Bus System

The performance of the proposed control is validated by Matlab simulations on the modified IEEE 34-bus distribution test system as shown in Fig. 3. The line parameters are adopted from [49] and the locations of DGs and loads are respectively indicated by stars and triangles in Fig. 3. For the droop-free control in [9], the α in (7) is set as 0 and the inequality constraints are removed and then the standard gradient decent algorithm [50] is used to solve the optimization problem.

1) Performance under load change: Fig. 10 shows the DG output voltages and reactive power under the proposed control with load change at 10 s. Fig. 11 shows the performance of the control in [9] for the same case. For the control in [9] the voltages range between 0.909 and 1.076 whereas the proposed control can bound the voltages between 0.95 and 1.05 and the normalized reactive power between 0.2 and 0.8.

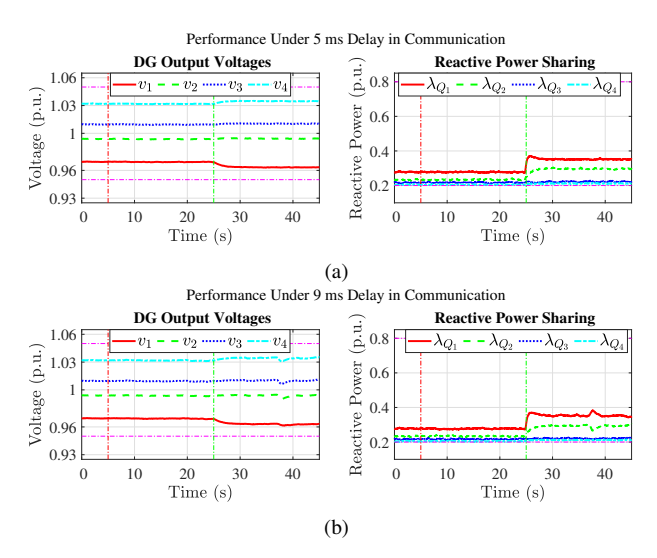


Fig. 9. Performance evaluation under communication delays. Communication delay is applied at 5 s and load change is applied at 25 s. (a) 5-ms delay; (b) 9-ms delay.

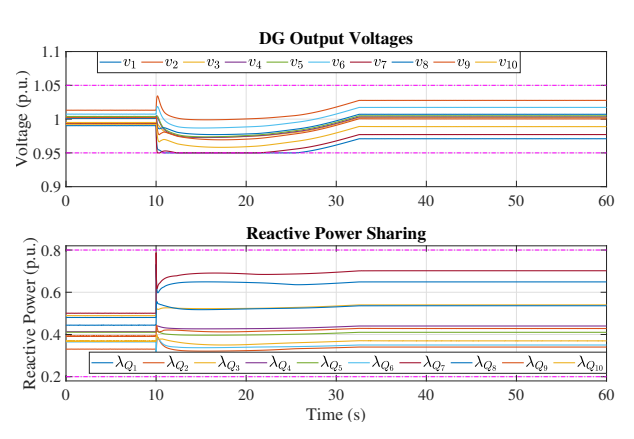


Fig. 10. Performance evaluation on the IEEE 34-bus test system for the proposed control. Load change is applied at $10~\rm s.$

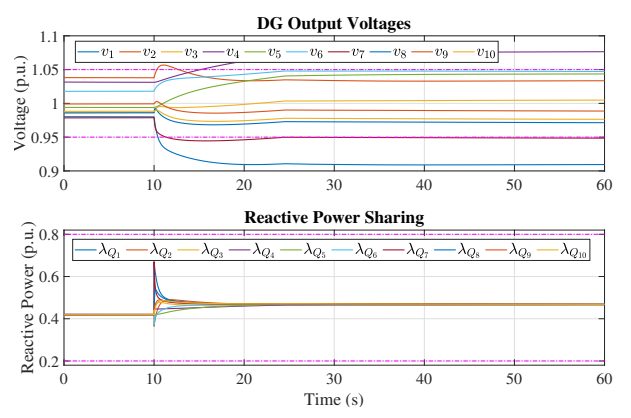


Fig. 11. Performance evaluation on the IEEE 34-bus test system for the control in [9]. Load change is applied at 10 s.

2) Performance under a wide range of load scenarios: The performance of the proposed control and the distributed control in [9] is compared under a wide range of load scenarios. We have generated 100 test cases in which each load is added a random change that follows a normal distribution with zero

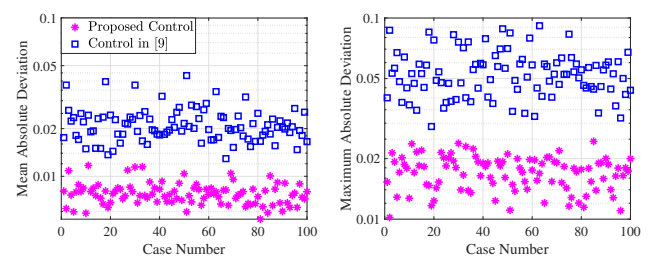


Fig. 12. Mean absolute deviations and maximum absolute deviations of DG output voltages for the proposed control and the control in [9].

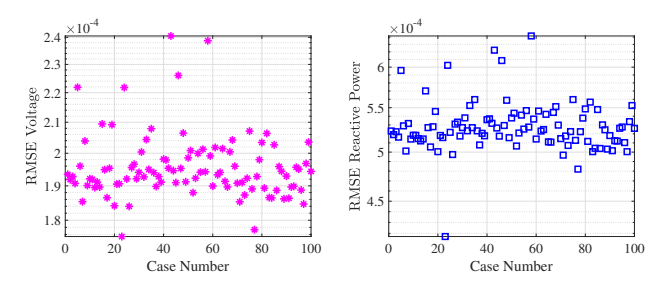


Fig. 13. RMSE of voltage and reactive power between centralized and distributed solution for 100 test cases under different load scenarios.

mean and a standard deviation as 10% of the initial load. The performance of the proposed controller and the controller in [9] is tested under these scenarios.

We have calculated the mean absolute deviation $\sum_{i=1}^{N} |v_i-1|/N$ and the maximum absolute deviation $\max(|\mathbf{v}-1|)$ of the DG output voltages for each case, which are shown in Fig. 12. For all test scenarios the mean and maximum absolute deviations with the proposed control are much less than those for the control in [9]. With the control in [9] the maximum voltage deviations for many cases are greater than 0.05 while the proposed control can always guarantee that the maximum voltage deviation is less than 0.05. This implies the proposed control can achieve better voltage profiles thanks to explicitly considering technical constraints and the proper coordination between voltage regulation and reactive power sharing.

- 3) Optimality comparison: The final steady-state obtained from the proposed distributed control is compared with a centralized optimization approach for different load scenarios. For the centralized approach we solve the optimization problem (10) using CPLEX [51] in Matlab YALMIP toolbox [52]. The root mean square error (RMSE) of the final steady-states for voltage and reactive power obtained from the proposed and the centralized approach under 100 load scenarios is shown in Fig. 13. In Fig. 14, the voltage and reactive power obtained from the proposed control and the centralized optimization approach are given respectively for case 43 and case 58 in Fig. 13 for which the voltage and reactive power RMSEs have the highest values. The results obtained from the proposed control are almost identical to those from the centralized approach.
- 4) Performance under line parameter uncertainty: In real power systems the line parameters may not be obtained accurately. Thus the performance of the proposed distributed control needs to be investigated under uncertainty in the line parameters. To validate robustness against line parameter uncertainty we consider 20 different load scenarios. For each

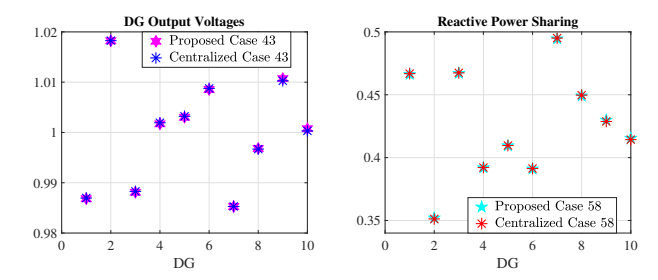


Fig. 14. DG output voltage and reactive power comparison between the centralized optimization and the proposed distributed control respectively for case 43 and case 58 in Fig. 13.

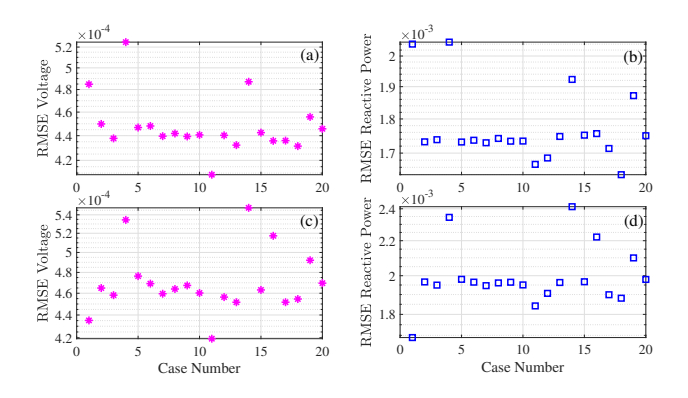


Fig. 15. RMSE of voltage and reactive power with 10 percent decrease or increase in line parameters under different loading conditions. (a) Voltage RMSE with 10 percent parameter decrease; (b) Reactive power RMSE with 10 percent parameter decrease; (c) Voltage RMSE with 10 percent parameter increase; and (d) Reactive power RMSE with 10 percent parameter decrease.

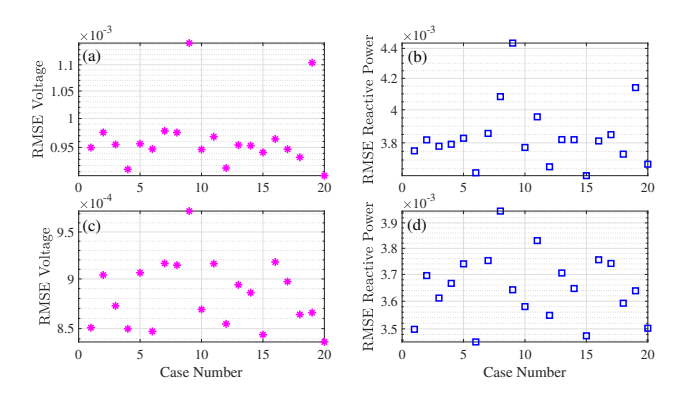


Fig. 16. RMSE of voltage and reactive power with 20 percent decrease or increase in line parameters under different loading conditions. (a) Voltage RMSE with 20 percent decrease; (b) Reactive power RMSE with 20 percent decrease; (c) Voltage RMSE with 20 percent increase; and (d) Reactive power RMSE with 20 percent decrease.

of the test cases we increase/decrease the true line parameters by 10% or 20% and compare with the actual solution without line parameter uncertainty. In Figs. 15 and 16, the RMSE of the steady-state voltage and reactive power respectively under 10% and 20% changes in the line parameters is shown. It can be seen that with higher line parameter uncertainty the RMSE will increase but is still small, indicating that the proposed control has robustness against line parameter uncertainties.

VI. CONCLUSION

In this paper, we propose an optimal distributed voltage control for grid-forming inverters in AC microgrids. The proposed control achieves an optimal trade-off between voltage regulation and reactive power sharing while obeying technical constraints on voltage and reactive power capacity. A distributed primal-dual gradient algorithm is developed to solve the formulated optimization problem. The proposed control and distributed solving algorithm are validated through simulations on the 4-DG and IEEE 34-bus systems.

Note that the existence and convergence analysis of the integrated optimization and dynamic consensus parts is a challenging problem and has not been provided in this paper. We will address this in our future work.

APPENDIX

The distributed estimator in (25) can be equivalently written in continuous time domain as [3], [4], [9]:

$$\hat{D}_{i}^{j}(t) = \frac{\partial \tilde{f}_{j}(\mathbf{v}(t))}{\partial v_{i}} + \int_{0}^{t} \sum_{k \in \mathcal{N}_{j}} a_{jk} \left(\hat{D}_{i}^{k}(\tau) - \hat{D}_{i}^{j}(\tau) \right) d\tau,$$

$$j = 1, \dots, N. \tag{35}$$

By differentiating (35) we have the following equation for DG j:

$$\dot{\hat{D}}_{i}^{j} = \dot{\hat{D}}_{i}^{j} + \sum_{k \in \mathcal{N}_{j}} a_{jk} \left(\hat{D}_{i}^{k} - \hat{D}_{i}^{j} \right)$$

$$= \dot{\tilde{D}}_{i}^{j} + \sum_{k \in \mathcal{N}_{i}} a_{jk} \hat{D}_{i}^{k} - d_{j}^{\text{in}} \hat{D}_{i}^{j}, \tag{36}$$

where $\tilde{D}_i^j = \partial \tilde{f}_i(\mathbf{v}(t))/\partial v_i$ and $d_j^{\text{in}} = \sum_{k \in \mathcal{N}_j} a_{jk}$ is the indegree of DG j. Accordingly, the global dynamics for DG i estimator \hat{D}_i^i can be written as:

$$\dot{\hat{\mathbf{D}}}_i = \dot{\hat{\mathbf{D}}}_i + \mathbf{A}\hat{\mathbf{D}}_i - \mathbf{D}^{\mathrm{in}}\hat{\mathbf{D}}_i = \dot{\hat{\mathbf{D}}}_i - \mathbf{L}\hat{\mathbf{D}}_i, \tag{37}$$

where $\hat{\mathbf{D}}_i = [\hat{D}_i^1, \hat{D}_i^2, \cdots, \hat{D}_i^N], \quad \tilde{\mathbf{D}}_i = [\partial \tilde{f}_1(\mathbf{v}(t))/\partial v_i, \partial \tilde{f}_2(\mathbf{v}(t))/\partial v_i, \cdots, \partial \tilde{f}_N(\mathbf{v}(t))/\partial v_i], \quad \mathbf{D}^{\text{in}}$ is the in-degree matrix, and \mathbf{L} is the Laplacian matrix of the communication network. Then in frequency domain (37) can be represented as:

$$s\hat{\mathbb{D}}_i - \hat{\mathbf{D}}_i(0) = s\tilde{\mathbb{D}}_i - \tilde{\mathbf{D}}_i(0) - \mathbf{L}\hat{\mathbb{D}}_i, \tag{38}$$

where $\hat{\mathbb{D}}_i$ and $\tilde{\mathbb{D}}_i$ represent the Laplace transform of $\hat{\mathbf{D}}_i$ and $\tilde{\mathbf{D}}_i$. Also from (35) we have $\hat{\mathbf{D}}_i(0) = \tilde{\mathbf{D}}_i(0)$. Then (38) can be rewritten as:

$$\hat{\mathbb{D}}_i = s(s\mathbf{I}_N + \mathbf{L})^{-1}\tilde{\mathbb{D}}_i,\tag{39}$$

where $\mathbf{I}_N \in \mathbb{R}^{N \times N}$ is an identity matrix.

Applying the final value theorem to (39), we have

$$\lim_{t \to \infty} \hat{\mathbf{D}}_i(t) = \lim_{s \to 0} s \hat{\mathbb{D}}_i = \lim_{s \to 0} s^2 (s \mathbf{I}_N + \mathbf{L})^{-1} \tilde{\mathbb{D}}_i.$$
 (40)

According to the Lemma A.2 of [4], if the communication network has an spanning tree and a balanced Laplacian matrix then we have

$$\lim_{s \to 0} s(s\mathbf{I}_N + \mathbf{L})^{-1} = \mathbf{M},\tag{41}$$

where $\mathbf{M} \in \mathbb{R}^{N \times N}$ is an averaging matrix with all the elements as (1/N). Then Eq. (40) becomes:

$$\lim_{t \to \infty} \hat{\mathbf{D}}_{i}(t) = \mathbf{M} \lim_{s \to 0} s \tilde{\mathbb{D}}_{i} = \mathbf{M} \lim_{t \to \infty} \tilde{\mathbf{D}}_{i}(t)$$

$$= \lim_{t \to \infty} \frac{1}{N} \sum_{i=1}^{N} \frac{\partial \tilde{f}_{j}(\mathbf{v}(t))}{\partial v_{i}} \mathbf{1}, \tag{42}$$

which implies that the estimated \hat{D}_i^j for $j=1,\ldots,N$ in (35) will converge to the true average value.

REFERENCES

- D. E. Olivares, A. Mehrizi-Sani, A. H. Etemadi, C. A. Cañizares, R. Iravani, M. Kazerani, A. H. Hajimiragha, O. Gomis-Bellmunt, M. Saeedifard, R. Palma-Behnke *et al.*, "Trends in microgrid control," *IEEE Trans. Smart Grid*, vol. 5, no. 4, pp. 1905–1919, Jul. 2014.
- [2] A. Bidram and A. Davoudi, "Hierarchical structure of microgrids control system," *IEEE Trans. Smart Grid*, vol. 3, no. 4, pp. 1963–1976, Dec. 2012.
- [3] S. M. Mohiuddin and J. Qi, "Droop-free distributed control for AC microgrids with precisely regulated voltage variance and admissible voltage profile guarantees," *IEEE Trans. Smart Grid*, vol. 11, no. 3, pp. 1956–1967, May 2020.
 [4] V. Nasirian, S. Moayedi, A. Davoudi, and F. L. Lewis, "Distributed
- [4] V. Nasirian, S. Moayedi, A. Davoudi, and F. L. Lewis, "Distributed cooperative control of DC microgrids," *IEEE Trans. Power Electron.*, vol. 30, no. 4, pp. 2288–2303, Apr. 2015.
- [5] V. Kekatos, L. Zhang, G. B. Giannakis, and R. Baldick, "Voltage regulation algorithms for multiphase power distribution grids," *IEEE Trans. Power Syst.*, vol. 31, no. 5, pp. 3913–3923, Sept. 2016.
- [6] S. Bolognani, R. Carli, G. Cavraro, and S. Zampieri, "On the need for communication for voltage regulation of power distribution grids," *IEEE Control Netw. Syst.*, vol. 6, no. 3, pp. 1111–1123, Sept. 2019.
- [7] S. M. Mohiuddin and J. Qi, "A unified droop-free distributed secondary control for grid-following and grid-forming inverters in AC microgrids," in *IEEE Power & Energy Society General Meeting*, Aug. 2020, pp. 1–5.
- [8] Y. Fan, G. Hu, and M. Egerstedt, "Distributed reactive power sharing control for microgrids with event-triggered communication," *IEEE Trans. Control Syst. Technol.*, vol. 25, no. 1, pp. 118–128, Jan. 2017.
- [9] V. Nasirian, Q. Shafiee, J. M. Guerrero, F. L. Lewis, and A. Davoudi, "Droop-free distributed control for AC microgrids," *IEEE Trans. Power Electron.*, vol. 31, no. 2, pp. 1600–1617, Feb. 2016.
- [10] N. Pogaku, M. Prodanovic, and T. C. Green, "Modeling, analysis and testing of autonomous operation of an inverter-based microgrid," *IEEE Trans. Power Electron.*, vol. 22, no. 2, pp. 613–625, Mar. 2007.
- [11] X. Wu, C. Shen, and R. Iravani, "A distributed, cooperative frequency and voltage control for microgrids," *IEEE Trans. Smart Grid*, vol. 9, no. 4, pp. 2764–2776, Jul. 2018.
- [12] A. H. Etemadi, E. J. Davison, and R. Iravani, "A decentralized robust control strategy for multi-DER microgrids—Part I: Fundamental concepts," *IEEE Trans. Power Del.*, vol. 27, no. 4, pp. 1843–1853, Oct. 2012.
- [13] H. Mahmood, D. Michaelson, and J. Jiang, "Reactive power sharing in islanded microgrids using adaptive voltage droop control," *IEEE Trans. Smart Grid*, vol. 6, no. 6, pp. 3052–3060, Nov. 2015.
- [14] R. Bhattarai, J. Qi, J. Wang, and S. Kamalasadan, "Adaptive droop control of coupled microgrids for enhanced power sharing and smallsignal stability," in 2020 IEEE Power & Energy Society General Meeting (PESGM). IEEE, Aug. 2020, pp. 1–5.
- [15] Y. Zhu, Q. Fan, B. Liu, and T. Wang, "An enhanced virtual impedance optimization method for reactive power sharing in microgrids," *IEEE Trans. Power Electron.*, vol. 33, no. 12, pp. 10390–10402, Dec. 2018.
- [16] Y. Han, H. Li, P. Shen, E. A. A. Coelho, and J. M. Guerrero, "Review of active and reactive power sharing strategies in hierarchical controlled microgrids," *IEEE Trans. Power Electron.*, vol. 32, no. 3, pp. 2427–2451, Mar. 2017.
- [17] A. Micallef, M. Apap, C. Spiteri-Staines, J. M. Guerrero, and J. C. Vasquez, "Reactive power sharing and voltage harmonic distortion compensation of droop controlled single phase islanded microgrids," *IEEE Trans. Smart Grid*, vol. 5, no. 3, pp. 1149–1158, May 2014.
- [18] M. S. Golsorkhi, Q. Shafiee, D. D. Lu, and J. M. Guerrero, "Distributed control of low-voltage resistive AC microgrids," *IEEE Trans. Energy Convers.*, vol. 34, no. 2, pp. 573–584, Jun. 2019.

- [19] M. Yazdanian and A. Mehrizi-Sani, "Distributed control techniques in microgrids," *IEEE Trans. Smart Grid*, vol. 5, no. 6, pp. 2901–2909, Nov. 2014
- [20] M. A. Shahab, B. Mozafari, S. Soleymani, N. M. Dehkordi, H. M. Shourkaei, and J. M. Guerrero, "Distributed consensus-based fault tolerant control of islanded microgrids," *IEEE Trans. Smart Grid*, vol. 11, no. 1, pp. 37–47, Jan. 2020.
- [21] S. M. Mohiuddin, J. Qi, S. Fung, Y. Huang, and Y. Tang, "Deep learning based multi-label attack detection for distributed control of ac microgrids," in *IEEE International Conference on Communications, Control,* and Computing Technologies for Smart Grids (SmartGridComm), Oct. 2021, pp. 233–238.
- [22] A. Nedich et al., "Convergence rate of distributed averaging dynamics and optimization in networks," Foundations and Trends® in Systems and Control, vol. 2, no. 1, pp. 1–100, 2015.
- [23] A. Bidram, V. Nasirian, A. Davoudi, and F. L. Lewis, Cooperative Synchronization in Distributed Microgrid Control. Springer, 2017.
- [24] F. L. Lewis, H. Zhang, K. Hengster-Movric, and A. Das, Cooperative control of multi-agent systems: optimal and adaptive design approaches. Springer Science & Business Media, 2013.
- [25] P. Lin, W. Ren, and J. A. Farrell, "Distributed continuous-time optimization: Nonuniform gradient gains, finite-time convergence, and convex constraint set," *IEEE Trans. Autom. Control*, vol. 62, no. 5, pp. 2239– 2253, 2017.
- [26] Y. Xu, H. Sun, W. Gu, Y. Xu, and Z. Li, "Optimal distributed control for secondary frequency and voltage regulation in an islanded microgrid," *IEEE Trans. Ind. Informat.*, vol. 15, no. 1, pp. 225–235, Jan. 2019.
- [27] H. Zhang, S. Kim, Q. Sun, and J. Zhou, "Distributed adaptive virtual impedance control for accurate reactive power sharing based on consensus control in microgrids," *IEEE Trans. Smart Grid*, vol. 8, no. 4, pp. 1749–1761, Jul. 2017.
- [28] J. W. Simpson-Porco, Q. Shafiee, F. Dörfler, J. C. Vasquez, J. M. Guerrero, and F. Bullo, "Secondary frequency and voltage control of islanded microgrids via distributed averaging," *IEEE Trans. Ind. Electron.*, vol. 62, no. 11, pp. 7025–7038, Nov. 2015.
- [29] R. Han, L. Meng, G. Ferrari-Trecate, E. A. A. Coelho, J. C. Vasquez, and J. M. Guerrero, "Containment and consensus-based distributed coordination control to achieve bounded voltage and precise reactive power sharing in islanded AC microgrids," *IEEE Trans. Ind. Appl.*, vol. 53, no. 6, pp. 5187–5199, Nov. 2017.
- [30] S. Magnússon, G. Qu, C. Fischione, and N. Li, "Voltage control using limited communication," *IEEE Control Netw. Syst.*, vol. 6, no. 3, pp. 993–1003, Sep. 2019.
- [31] G. Qu and N. Li, "Optimal distributed feedback voltage control under limited reactive power," *IEEE Trans. Power Syst.*, vol. 35, no. 1, pp. 315–331, Jan. 2020.
- [32] H. J. Liu, W. Shi, and H. Zhu, "Hybrid voltage control in distribution networks under limited communication rates," *IEEE Trans. Smart Grid*, vol. 10, no. 3, pp. 2416–2427, May 2019.
- [33] H. Zhang, F. L. Lewis, and Z. Qu, "Lyapunov, adaptive, and optimal design techniques for cooperative systems on directed communication graphs," *IEEE Trans. Ind. Electron.*, vol. 59, no. 7, pp. 3026–3041, Jul. 2012.
- [34] A. Floriduz, M. Tucci, S. Riverso, and G. Ferrari-Trecate, "Approximate kron reduction methods for electrical networks with applications to plugand-play control of ac islanded microgrids," *IEEE Trans. Control Syst. Technol.*, vol. 27, no. 6, pp. 2403–2416, Nov. 2019.
- [35] W. H. Kersting, Distribution system modeling and analysis. CRC press, 2006.
- [36] J. Yang, N. Zhang, C. Kang, and Q. Xia, "A state-independent linear power flow model with accurate estimation of voltage magnitude," *IEEE Trans. Power Syst.*, vol. 32, no. 5, pp. 3607–3617, Sept. 2017.
- [37] S. Liang, X. Zeng, and Y. Hong, "Distributed nonsmooth optimization with coupled inequality constraints via modified Lagrangian function," *IEEE Trans. Autom. Control*, vol. 63, no. 6, pp. 1753–1759, Jun. 2018.
- [38] P. Yi, Y. Hong, and F. Liu, "Initialization-free distributed algorithms for optimal resource allocation with feasibility constraints and application to economic dispatch of power systems," *Automatica*, vol. 74, pp. 259–269, Dec. 2016.
- [39] A. Nedić and A. Ozdaglar, "Subgradient methods for saddle-point problems," *Journal of optimization theory and applications*, vol. 142, no. 1, pp. 205–228, Jul. 2009.
- [40] M. Zhu and S. Martinez, "On distributed convex optimization under inequality and equality constraints," *IEEE Trans. Autom. Control*, vol. 57, no. 1, pp. 151–164, Jan. 2012.
- [41] Y. Nesterov, Introductory lectures on convex optimization: A basic course. Springer Science & Business Media, Dec. 2013, vol. 87.

- [42] P. Di Lorenzo and G. Scutari, "NEXT: In-network nonconvex optimization," *IEEE Trans. Signal Inf. Process. Netw.*, vol. 2, no. 2, pp. 120–136, Feb. 2016.
- [43] D. P. Spanos, R. Olfati-Saber, and R. M. Murray, "Dynamic consensus on mobile networks," in *Proc. 16th Int. Fed. Autom. Control*, 2005, pp. 1–6.
- [44] S. Zhang, C. Tepedelenlioglu, A. Spanias, and M. K. Banavar, "Node counting in wireless sensor networks," in 2015 49th Asilomar Conference on Signals, Systems and Computers, 2015, pp. 360–364.
- [45] V. Kekatos and G. B. Giannakis, "Distributed robust power system state estimation," *IEEE Trans. Power Syst.*, vol. 28, no. 2, pp. 1617–1626, 2013
- [46] H. Xu, A. D. Domínguez-García, V. V. Veeravalli, and P. W. Sauer, "Data-driven voltage regulation in radial power distribution systems," *IEEE Trans. Power Syst.*, vol. 35, no. 3, pp. 2133–2143, 2020.
- [47] A. Yazdani and R. Iravani, *Voltage-sourced converters in power systems:* modeling, control, and applications. John Wiley & Sons, 2010.
- [48] Q. Huang and V. Vittal, "Advanced EMT and phasor-domain hybrid simulation with simulation mode switching capability for transmission and distribution systems," *IEEE Trans. Power Syst.*, vol. 33, no. 6, pp. 6298–6308, May 2018.
- [49] N. Mwakabuta and A. Sekar, "Comparative study of the IEEE 34 node test feeder under practical simplifications," in *Proc. 39th North Amer. Power Symp.*, 2007, pp. 484–491.
- [50] S. Boyd, N. Parikh, E. Chu, B. Peleato, and J. Eckstein, "Distributed optimization and statistical learning via the alternating direction method of multipliers," *Found. Trends Mach. Learn.*, vol. 3, pp. 1–122, 2010.
- [51] IBM ILOG CPLEX, "V12. 1: User's manual for CPLEX," *International Business Machines Corporation*, vol. 46, no. 53, p. 157, 2009.
- [52] J. Löfberg, "YALMIP: A toolbox for modeling and optimization in matlab," in *In Proceedings of the CACSD Conference*, Taipei, Taiwan, 2004



Sheik M. Mohiuddin (S'16) received the B.Sc. degree in Electrical and Electronic Engineering, from Rajshahi University of Engineering & Technology, Bangladesh, in 2013 and Masters in Electrical Engineering from University of New South Wales (UNSW), Australia, in 2017, and he is currently pursuing the Ph.D. degree in electrical engineering with Stevens Institute of Technology under the supervision of Dr. J. Qi. He was a Research Assistant at Deakin University, Australia from September 2017–December 2017. He worked as a Summer Student

Assistant at Brookhaven National Laboratory, USA from May 2021 to August 2021. His research interests include distributed control for grid-forming and grid-feeding converters in the AC/DC microgrid, distributed control for hybrid PV energy storage, state estimation, hardware in the loop simulation, and cybersecurity in the microgrid.



Junjian Qi (S'12–M'13–SM'17) received the B.E. degree in electrical engineering, from Shandong University, Jinan, China, in 2008, and the Ph.D. degree in electrical engineering from Tsinghua University, Beijing, China, in 2013. He was a Visiting Scholar with Iowa State University, Ames, IA, USA, in 2012, a Research Associate with the Department of EECS, University of Tennessee, Knoxville, TN, USA, from 2013 to 2015, a Postdoctoral Appointee with the Energy Systems Division, Argonne National Laboratory, Lemont, IL, USA, from 2015 to 2017,

and an Assistant Professor with the Department of Electrical and Computer Engineering, University of Central Florida, Orlando, FL, USA, from 2017 to 2020. He is currently an Assistant Professor with the Department of Electrical and Computer Engineering, Stevens Institute of Technology, Hoboken, NJ, USA. He was the recipient of the NSF CAREER award in 2020 and is an Associate Editor for IET Generation, Transmission & Distribution and IEEE Access. His research interests include cascading blackouts, microgrid control, cyber-physical systems, and synchrophasors.